Bull. Mater. Sci., Vol. 34, No. 6, October 2011, pp. 1257–1262. © Indian Academy of Sciences.

$Ba_3(P_{1-x}Mn_xO_4)_2$: Blue/green inorganic materials based on tetrahedral Mn(V)

SOURAV LAHA, ROHIT SHARMA, S V BHAT†, M L P REDDY‡, J GOPALAKRISHNAN* and S NATARAJAN

Solid State and Structural Chemistry Unit, †Department of Physics, Indian Institute of Science, Bangalore 560 012, India
‡Chemical Science and Technology Division, National Institute for Interdisciplinary Science and Technology (NIIST), Thiruvananthapuram 695 019, India

MS received 11 May 2011

Abstract. **We describe a blue/green inorganic material, $Ba_3(P_{1-x}Mn_xO_4)_2$ (I) based on tetrahedral MnO_4^{3-}:$3d^2$ chromophore. The solid solutions (I) which are sky-blue and turquoise-blue for $x \leq 0{\cdot}25$ and dark green for $x \geq 0{\cdot}50$, are readily synthesized in air from commonly available starting materials, stabilizing the MnO_4^{3-} chromophore in an isostructural phosphate host. We suggest that the covalency/ionicity of P–O/Mn–O bonds in the solid solutions tunes the crystal field strength around Mn(V) such that a blue colour results for materials with small values of x. The material could serve as a nontoxic blue/green inorganic pigment.**

Keywords. **Blue/green inorganic material; barium phosphate/manganate(V); tetrahedral manganate(V); blue/green chromophore; ligand field tuning of colour.**

1. Introduction

Inorganic solids displaying bright colours are important as pigment materials which find a wide range of applications in paints, inks, plastics, rubbers, ceramics, enamels and glasses (Buxbaum and Pfaff 2005). From a scientific standpoint, there are atleast three different mechanisms by which inorganic solids acquire colour: (i) electronic interband transitions in the visible (Jansen and Letschert 2000; Dolgos *et al* 2009) as for example in the recently discovered yellow-red pigments based on perovskite, (Ca,La)Ta(O,N)$_3$ (Jansen and Letschert 2000), (ii) intervalence charge-transfer between transition metal ions as in the blue sapphire (Fe^{2+}–Ti^{4+} charge-transfer in α-Al_2O_3 host) (http://en.wikipedia.org/wiki/Sapphire) and (iii) crystal field transitions as in the well known ruby (octahedrally coordinated Cr^{3+} in α-Al_2O_3) (Esposti and Bizzocchi 2007).

Among the three primary colours (red, green and blue) that produce different shades of colours in inorganic solids, blue coloured pigment quality materials are relatively rare. Some of the common blue pigments of inorganic origin are : azurite [$Cu_3(CO_3)_2(OH)_2$], Egyptian blue ($CaCuSi_4O_{10}$), Prussian blue ($Fe_4[Fe(CN_6)]_3$), and ultramarine ($Na_7Al_6Si_6O_{24}S_3$). $YIn_{1-x}Mn_xO_3$ is a recently developed blue pigment (Smith *et al* 2009) that derives its colour from crystal field transitions within an unusual five coordinated trigonal bipyramidal Mn(III). A turquoise-blue solid based on $Li_{1{\cdot}33}Ti_{1{\cdot}66}O_4$ spinel oxide wherein the colour arises from an intervalence charge-transfer between Ti^{3+} and Ti^{4+} has also been described recently (Fernández-Osorio *et al* 2011). Considering the paucity of blue/green inorganic solids that are colour-stable, environmentally benign and nontoxic, as well as readily synthesized from cost-effective commonly available constituents, we perceived the need to develop new blue or blue–green inorganic pigment-quality materials. Towards this end, we identified tetrahedral Mn(V): MnO_4^{3-} as a blue-green chromophore that could be readily stabilized in a barium phosphate lattice. While the Mn(V):MnO_4^{3-} ion is known to be stable in several alkaline earth phosphate lattices (Kingsley *et al* 1965; Borromei *et al* 1981; Dardenne *et al* 1998), we found that $Ba_3(PO_4)_2$ is a convenient matrix for developing a blue/green pigment based on Mn(V):MnO_4^{3-}, inasmuch as both $Ba_3(PO_4)_2$ (white) and $Ba_3(MnO_4)_2$ (intense green) are isostructural (Zachariasen 1948; Sugiyama and Tokonami 1990; Weller and Skinner 1999), crystallizing in a hexagonal *R–3m* structure that contains discrete PO_4/MnO_4 tetrahedra. MnO_4^{3-} acts as the chromophore in the isostructural solid solutions between $Ba_3(PO_4)_2$ and $Ba_3(MnO_4)_2$, where we are able to tune the colour from sky-blue for low concentrations of Mn to turquoise blue and to dark green with increasing Mn concentration across the series, $Ba_3(P_{1-x}Mn_xO_4)_2$. The synthesis and characterization of structure and optical properties of this material identifying the lattice tuning of colour are described in this paper.

*Author for correspondence (gopal@sscu.iisc.ernet.in)

2. Experimental

2.1 *Sample preparation*

$Ba_3(P_{1-x}Mn_xO_4)_2$ ($x = 0, 0{\cdot}02, 0{\cdot}05, 0{\cdot}10, 0{\cdot}25, 0{\cdot}30, 0{\cdot}40, 0{\cdot}50, 0{\cdot}75, 0{\cdot}90$ and $1{\cdot}00$) compounds were prepared by conventional ceramic method. For this purpose, high purity $BaCO_3$, $(NH_4)H_2PO_4$ and $MnC_2O_4{\cdot}2H_2O$ were mixed in stoichiometric proportions and the mixtures heated first at 400°C for 4 h, followed by heating at 950°C with intermittent grindings. The duration of the 950°C heating depends on the composition. Thus, for 2% and 5% Mn doping, a heating of 12 h × 2 was adequate. Higher concentration of Mn doping required longer heating times (up to 12 h × 7) at 950°C.

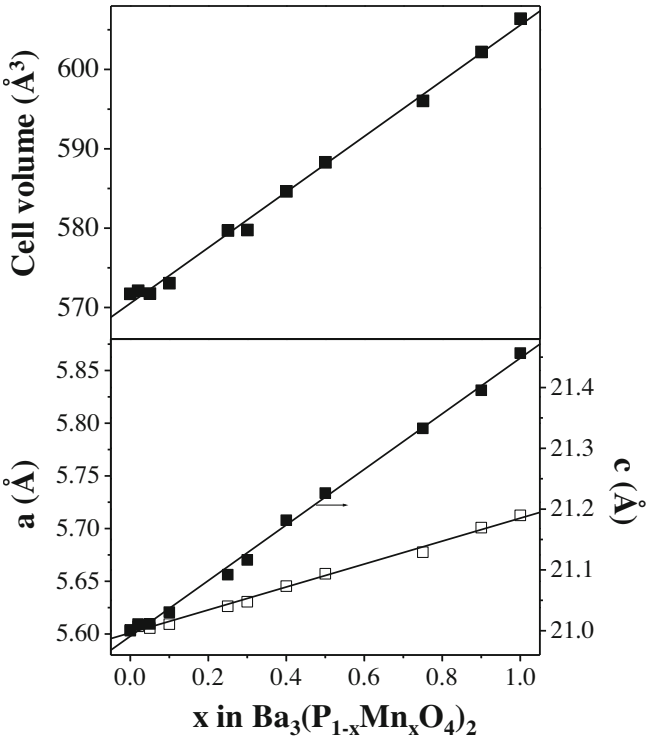

Figure 1. Unit cell parameters of $Ba_3(P_{1-x}Mn_xO_4)_2$ solid solutions: (bottom) a and c and (top) cell volume.

2.2 *Experimental techniques*

Formation of single-phase products and their crystal structure were studied by powder X-ray diffraction (PXRD). PXRD patterns were recorded with a Philips X'pert Diffractometer (Ni-filtered Cu Kα radiation, $\lambda = 1{\cdot}5418$ Å). PXRD patterns were simulated by the program POWDERCELL (Kraus and Nolze 1996). Cell parameters were determined by Le Bail fitting of the data by means of the program GSAS (Larson and Von Dreele 1990). PXRD data for Rietveld refinement of the structures were collected at room temperature employing the same diffractometer in the 2θ range 20–60° with a step size of 0·02° and step duration, 25 s. The refinement was carried out by means of the program GSAS (Larson and Von Dreele 1990). A sixth order Chebychev polynomial for the background, zero, LP factor, scale, pseudo-Voigt profile function (U, V, W and X), lattice parameters, atomic parameters, and U_{iso} (total 23 parameters) were used in refinement. The thermal parameters were constrained to be the same for atoms occupying the same site (Mn and P).

Diffuse reflectance spectra of powdered samples were recorded by means of a Perkin Elmer Lambda 750 UV-vis spectrometer in 300–1300 nm range. For characterization of pigment quality of the samples (the colour parameters), the diffuse reflectance spectra were recorded (380–780 nm)

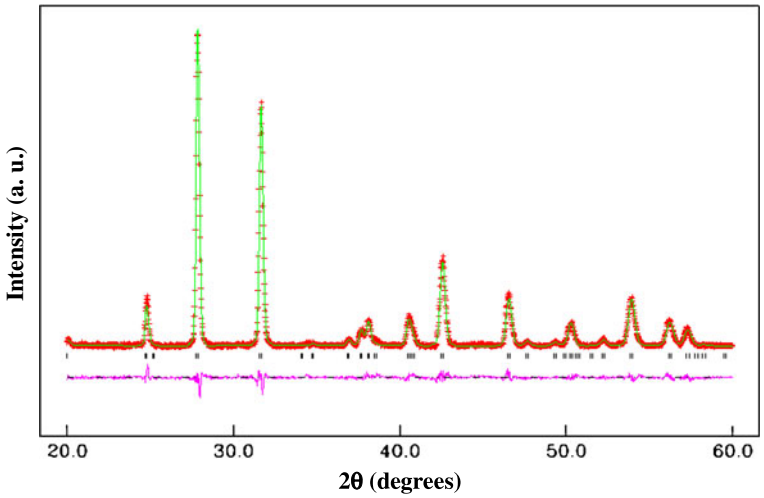

Figure 2. Rietveld refinement of structure of $Ba_3(P_{0{\cdot}25}Mn_{0{\cdot}75}O_4)_2$ from powder XRD data. Observed (+), calculated (−) and difference (bottom) profiles are shown. Vertical bars indicate position of Bragg reflections.

Table 1. Crystallographic data for $Ba_3(P_{0.25}Mn_{0.75}O_4)_2$ [space group *R–3m*, $a = 5{\cdot}6773(1)$ Å, $c = 21{\cdot}3156(7)$ Å] together with selected bond lengths.

Atom	Site	x	y	z	U_{iso}	Occupancy
Ba1	3a	0	0	0	0·033(2)	1
Ba2	6c	0	0	0·2076(1)	0·017(1)	1
P	6c	0	0	0·4070(1)	0·010(2)	0·25
Mn	6c	0	0	0·4070(1)	0·010(2)	0·75
O1	6c	0	0	0·3292(1)	0·024(8)	1
O2	18h	0·163(1)	0·326(2)	0·5653(5)	0·012(4)	1

Reliability factors: $R_p = 7{\cdot}59$, $R_{wp} = 10{\cdot}95$, $R_F^2 = 7{\cdot}00$, $\chi^2 = 1{\cdot}753$; bond lengths (Å): Ba(1) − O(1) = 3·279 (1)(×6); Ba(1) − O(2) = 2·730 (1)(×6); Ba(2) − O(1) = 2·591(3); Ba(2) − O(2) = 2·886(2)(×6); Ba(2) − O(2) = 2·763 (1)(×3); P/Mn − O(1) = 1·660(1); P/Mn − O(2) = 1·710(1)(×3)

employing a Shimadzu UV-2450 UV-vis spectrometer equipped with an integrating sphere attachment, ISR-2200. The measurements were made with an illuminant D_{65}, 10° complementary observer and measuring geometry $d/8°$. The colour parameters were determined by an analytical software (UVPC Colour Analysis Personal Spectroscopy Software V3, Shimadzu) coupled to the UV-2450 spectrometer. The CIE 1976 $L^*a^*b^*$ colorimetric method was used, as recommended by the Commission Internationale de l'Eclairage (CIE). In this method, L^* is the lightness axis [black (0) to white (100)], a^* is the green (−ve) to red (+ve) axis, and b^* is the blue (−ve) to yellow (+ve) axis. The parameter, C^* (chroma) represents saturation of the colour and h^o represents the hue angle. For each colorimetric parameter of the sample, measurement was made in triplicate and the average value was chosen as a result. Typically, for a given sample, the standard deviation of the measured CIE – $L^*a^*b^*$ values is <0·10, and the relative standard deviation is not >1%. Infrared spectra were recorded in KBr pellets with a Perkin Elmer SPECTRUM 1000 spectrometer from 400–1200 cm^{-1}. A Bruker X-band EMX spectrometer was employed to record the EPR spectra in the interval of 2000–5000 Gauss.

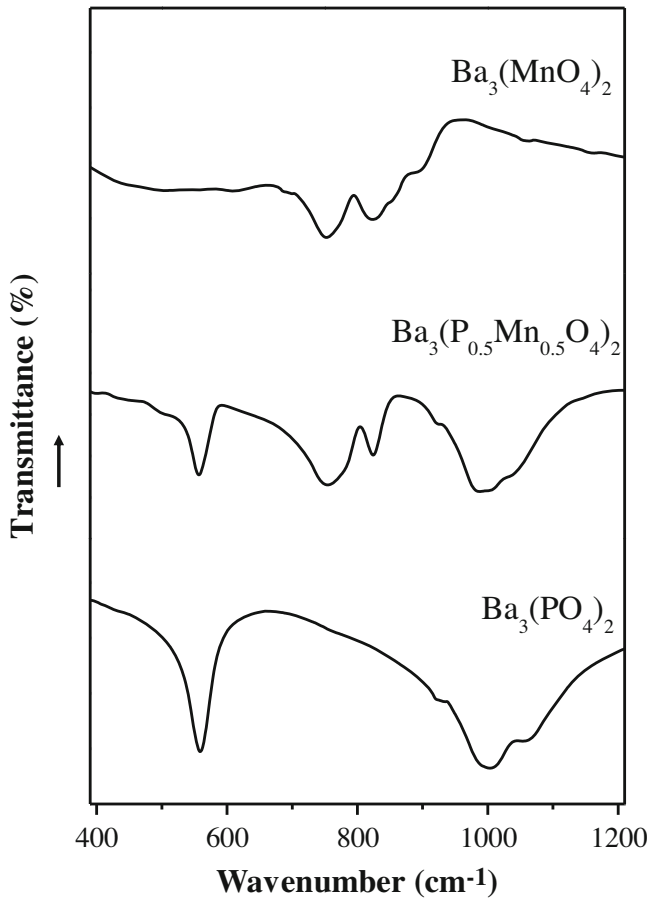

Figure 3. Infrared (IR) absorption spectra.

3. Results and discussion

3.1 *Composition and crystal structure*

We could readily prepare the solid solutions, $Ba_3(P_{1-x}Mn_xO_4)_2$ for $0 \leq x \leq 1{\cdot}0$, by the conventional ceramic method from commonly available starting materials, $BaCO_3$, $(NH_4)H_2PO_4$ and $MnC_2O_4{\cdot}2H_2O$ by carrying out the synthesis at 600–950°C in air. Under these conditions, manganese is stabilized in the (V) oxidation state, facilitating the formation of the isostructural solid solutions. Indeed, both the redox titration and EPR spectra reveal that manganese occurs in the (V) state. A single, nearly Lorentzian signal was obtained around $g = 1{\cdot}9736$. The absence of fine and hyperfine structure indicates a strong exchange narrowing, as observed in the case of Li_3MnO_4 with $g = 1{\cdot}9780$ (Sharmann *et al* 1975). Based on the similarities with the signal in Li_3MnO_4, EPR result indicates the presence of Mn(V) in the solid solutions.

PXRD patterns reveal that all the members of $Ba_3(P_{1-x}Mn_xO_4)_2$ are isostructural, adopting the hexagonal

R–3m structure of the end members. Least squares refined lattice parameters show a systematic increase with increasing x (figure 1) indicating Vegard's law behaviour, consistent with the tetrahedral ionic radii (Shannon 1976) of Mn(V) (0·33 Å) and P(V) (0·17 Å).

Refinement of the crystal structure of representative members of the solid solutions (figure 2, table 1) affirms the occurrence of the parent *R–3m* structure for the solid solutions, where the P/Mn–O bonds retain the slightly distorted tetrahedral geometry (C_{3v}) as in the parent end members. Infrared (IR) absorption spectra (figure 3) reveal the presence of discrete PO_4^{3-} and MnO_4^{3-} units in the solid solutions, the absorption bands (ν_3 and ν_4) for the PO_4^{3-} and (ν_3) for the MnO_4^{3-}, occurring nearly at the same frequency as in the parents (Baran and Manca 1982).

3.2 *Colours and diffuse reflectance spectra*

The change in colour of the samples, as seen by the naked eye (figure 4) and also as shown by the CIE $L^*a^*b^*$ chromatic parameters b^* (blue), a^* (green) as well as L^* (brightness) (table 2) for the selected compositions is striking: while the end members are white [$Ba_3(PO_4)_2$] and dark green [$Ba_3(MnO_4)_2$], the colour of the solid solutions changes from sky blue ($x = 0{\cdot}02$–$0{\cdot}10$), to turquoise blue ($x = 0{\cdot}25$–$0{\cdot}40$) to green and dark green ($x \geq 0{\cdot}50$) across the series.

The diffuse reflectance spectra (figure 5) reveal the origin of colour and its change across the series: while the parent phosphate, $Ba_3(PO_4)_2$, has practically no absorption in the visible, consistent with its white colour, the parent manganate, $Ba_3(MnO_4)_2$, shows a broad envelope of

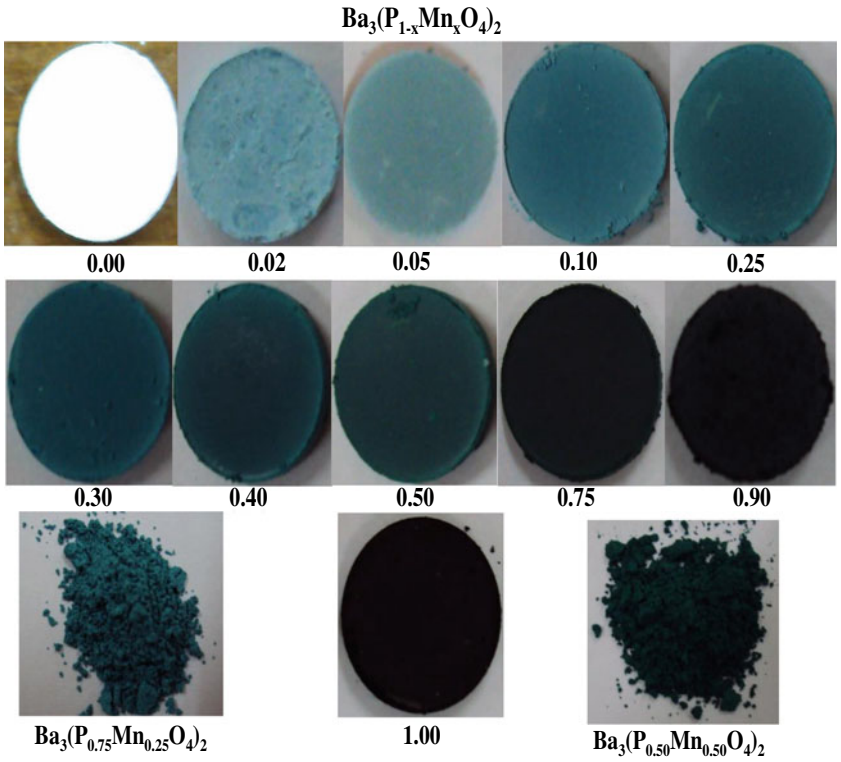

Figure 4. Colour of $Ba_3(P_{1-x}Mn_xO_4)_2$. Colours of both pellets and powder are shown.

Table 2. Colour coordinates (±0·1) for $Ba_3(P_{1-x}Mn_xO_4)_2$.

Compounds	Colour coordinates				
	L^*	a^*	b^*	C^*	H^o
$Ba_3(P_{0.98}Mn_{0.02}O_4)_2$	82·47	−14·80	−6·68	16·24	204
$Ba_3(P_{0.95}Mn_{0.05}O_4)_2$	76·78	−22·31	−9·95	24·43	204
$Ba_3(P_{0.90}Mn_{0.10}O_4)_2$	70·80	−27·95	−10·50	29·86	201
$Ba_3(P_{0.60}Mn_{0.40}O_4)_2$	52·07	−42·56	−7·56	43·22	190
$Ba_3(MnO_4)_2$	30·25	−25·52	5·91	26·19	167

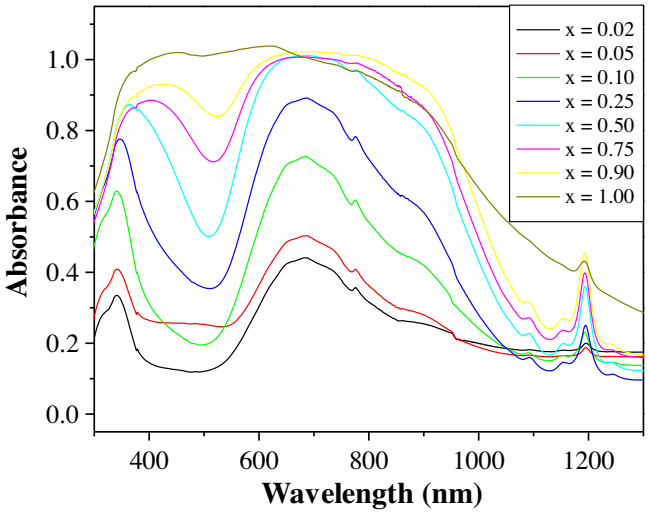

Figure 5. Diffuse reflectance spectra of $Ba_3(P_{1-x}Mn_xO_4)_2$ members.

absorption covering the entire visible region. There are two broad absorption maxima around 450 nm and 600 nm, with a shallow minimum around 500 nm consistent with its dark green colour. For small values of x (0·02–0·05), we see two distinct absorption maxima centred around 340 and 680 nm which progressively became intense and broader moving towards each other as x (Mn content) increases.

Clearly, the broad absorption centred around 680 nm together with the absence of absorption in the 400–550 nm region for $x \leq 0{\cdot}25$ results in blue colour. For $x \geq 0{\cdot}50$, broadening and shifting of the 680 nm absorption band together with the decrease/disappearance of the absorption minimum in the 400–550 nm region with increasing x changes the colour of the samples progressively from blue to dark green. A similar colour change has been reported for MnO_4^{3-} in phosphates of spodiosite structure (Lachwa and Reinen 1989), but its potential for the development of blue pigment was not explored.

The optical absorption spectrum of $3d^2$:MnO_4^{3-} ion has been investigated in several isomorphic phosphate/vanadate lattices (Kingsley *et al* 1965; Borromei *et al* 1981; Scott *et al* 1997; Dardenne *et al* 1998). Five transitions are observed in the spectral range 300–1300 nm : they are the three spin allowed absorptions from the $^3A_2$ ground state to $^3T_2$, $^3T_1(^3F)$ and $^3T_1(^3P)$ and two spin forbidden absorptions corresponding to $^3A_2 \rightarrow {}^1A_1$ and $^3A_2 \rightarrow {}^1E$ transitions. It must, however, be remembered that for a perfect T_d symmetry, only the $^3A_2 \rightarrow {}^3T_1(^3F)$ transition is allowed. In addition, the ligand(L) – metal(M) charge transfer absorption occurs at <400 nm in the UV range. We could identify all the five ligand field electronic transitions as well as the charge transfer absorption in the $Ba_3(PO_4)_2$ – $Ba_3(MnO_4)_2$ solid solutions, especially with low Mn concentrations. We assign the absorption bands for the $x = 0{\cdot}25$ member in figure 6. We estimate the Dq value from the $^3A_2 \rightarrow {}^3T_2$ transition to be 1120 cm^{-1}. The value compares favourably with the reported Dq value of MnO_4^{3-} in Ca_2PO_4Cl (Kingsley *et al* 1965; Borromei *et al* 1981), $Ba_5(PO_4)_3F$ (Dardenne *et al* 1998) and $Sr_5(VO_4)_3F$ (Scott *et al* 1997). The spin forbidden bands to ^1E and $^1A_1$ states at ∼775 nm (∼12900 cm^{-1}) and ∼1200 nm (∼8330 cm^{-1}) are most likely the zero phonon transitions from the $^3A_2$ ground state, suggesting the substitution of Mn(V) for P(V) in the solid solutions, as reported for $Ba_5(PO_4)_3F$:Mn (V).

The blue colour and its change to dark green across the solid solution series, $Ba_3(P_{1-x}Mn_xO_4)_2$, could be understood in the light of the optical absorption spectra (figure 4). As already pointed out, the strong absorption maxima at 340 and 680 nm together with the shallow minimum in the 400–550 nm results in the desired sky/turquoise blue colour for the materials with $x \leq 0{\cdot}25$. The occurrence of a robust blue colour (table 2) suggests that the materials could be useful as a 'blue pigment'. For $x > 0{\cdot}25$, the absorption band becomes broader owing to the increasing concentration of Mn(V) chromophore in the lattice changing the colour to green. However, shift of the 650 nm absorption maximum towards shorter wavelengths for increasing Mn(V), implying an increase of the ligand field strength, is not easy to understand. Since the P – O bonds in $Ba_3(PO_4)_2$ are shorter than the Mn(V) – O bonds in $Ba_3(MnO_4)_2$, one would expect that the Mn(V) substituted for P in $Ba_3(PO_4)_2$ host experiences a larger crystal field for small values of x in $Ba_3(P_{1-x}Mn_xO_4)_2$ than in the parent $Ba_3(MnO_4)_2$. Accordingly, one would have expected the ligand field transitions to move to shorter wavelengths for small values of x. However, the experimental results are to the contrary: for small values of x, the ligand field absorption moves to longer wavelengths. A likely explanation for this observation could be

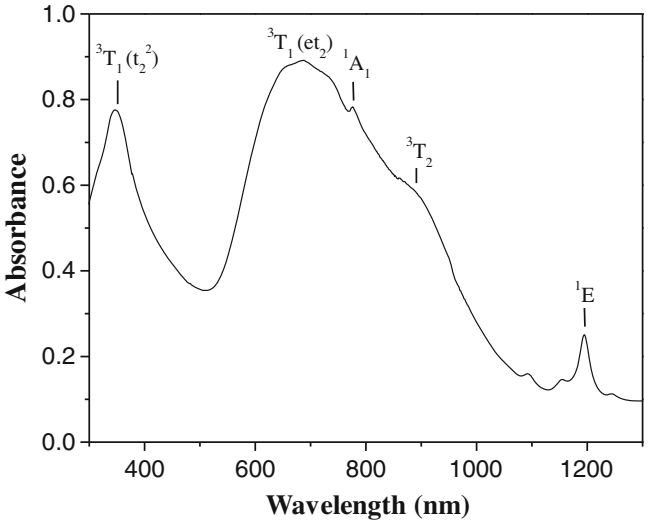

Figure 6. Assignment of optical absorption bands of MnO_4^{3-} in $Ba_3(P_{0.75}Mn_{0.25}O_4)_2$. Transitions from $^3A_2$ as ground state to various excited states are identified in spectrum.

that the Mn(V) substituted for P(V) in $Ba_3(PO_4)_2$ experiences a smaller crystal field strength for small values of x, because of a larger covalency of the P – O bonds; the latter would leave a smaller negative charge on the oxygens. With increasing x, the P/Mn – O bonds would become progressively more ionic, increasing the crystal field strength around Mn(V) thus shifting the *d–d* absorption towards smaller wavelengths. Further experimental work probing the actual charge on the oxygens is required to support this explanation.

4. Conclusions

We have synthesized a new blue/green inorganic material, $Ba_3(P_{1-x}Mn_xO_4)_2$, based on tetrahedral MnO_4^{3-}:$3d^2$ chromophore, which shows a robust sky blue and turquoise blue colour for $x \leq 0{\cdot}25$. For large values of x, the colour changes to dark green, approaching that of the parent $Ba_3(MnO_4)_2$. Accordingly, we have identified tetrahedral MnO_4^{3-} as new chromophore that gives blue and green colours when doped in an isomorphous phosphate host. We have argued that the occurrence of blue colour is likely due to a smaller crystal field strength experienced by Mn (V) in $Ba_3(PO_4)_2$ than in the parent $Ba_3(MnO_4)_2$. Considering that there are only a handful of blue inorganic pigments that are robust, cost-effective and environmentally benign, we believe the present work is significant and deserves further attention.

Acknowledgements

One of the authors (JG) thanks the Indian National Science Academy, New Delhi, for the award of a Senior Scientist position. (JG) and (SN) thank the Department of Science and Technology, Government of India, for the award of a Ramanna Fellowship.

References

Baran E J and Manca S G 1982 *Spectrosc. Letts* **15** 455
Borromei R, Oleari L and Day P 1981 *J. Chem. Soc., Faraday Trans.* **77** 1563
Buxbaum G and Pfaff G (eds) 2005 *Industrial inorganic pigments* (Weinheim: Wiley-VCH) 3rd ed.
Dardenne K, Vivien D, Ribot F, Chottard G and Huguenin D 1998 *Eur. J. Solid State Inorg. Chem.* **35** 419
Dolgos M R, Paraskos A M, Stoltzfus M W, Yarnell S C and Woodward P M 2009 *J. Solid State Chem.* **182** 1964
Esposti C D and Bizzocchi L 2007 *J. Chem. Educ.* **84** 1316
Fernández-Osorio A, Jiménez-Segura M P, Vázquez-Olmos A and Sato-Berru R 2011 *Ceram. Int.* **37** 1465
http://en.wikipedia.org/wiki/Sapphire
Jansen M and Letschert H P 2000 *Nature* **404** 980
Kingsley J D, Prener J S and Segall B 1965 *Phys. Rev.* **A137** 189
Kraus W and Nolze G 1996 *J. Appl. Crystallogr.* **29** 301
Lachwa H and Reinen D 1989 *Inorg. Chem.* **28** 1044
Larson A C and Von Dreele R B 1990 General structure analysis system, report LAUR, Los Alamos National Laboratory, Los Alamos, NM, p. 86
Scott M A, Henderson B, Gallagher H G and Han T P J 1997 *J. Phys: Condens. Matter* **9** 9893
Shannon R D 1976 *Acta Crystallogr.* **A32** 751
Sharmann A, Vitt B, Hoppe R. and Meyer G 1975 *Phys. Status Solidi (b)* **72** 197
Smith A E, Mizoguchi H, Delaney K, Spaldin N A, Sleight A W and Subramanian M A 2009 *J. Am. Chem. Soc.* **131** 17084
Sugiyama K and Tokonami M 1990 *Mineral. J.* **15** 141
Weller M T and Skinner S J 1999 *Acta Crystallogr.* **C55** 154
Zachariasen W H 1948 *Acta Crystallogr.* **1** 263